International Journal of Heat and Technology
Vol. 37, No. 3, September, 2019, pp. 766-778
Journal homepage: http://iieta.org/journals/ijht

Variable Fluid Property for MHD Viscous Fluid Containing Gyrotactic Microorganisms Flow over a Permeable Stretching Sheet

Manjeet Kumari[1*], Shalini Jain[2]

[1] Dept. of Mathematics & Statistics, Manipal University Jaipur, Jaipur 302026, Rajasthan, India
[2] Dept. of Mathematics, University of Rajasthan, Jaipur 302004, Rajasthan, India

Corresponding Author Email: manjeetyadav.muj@gmail.com

https://doi.org/10.18280/ijht.370313

Received: 25 July 2018
Accepted: 20 August 2019

Keywords:
first and second order velocity slip, temperature jump, concentration slip, microorganism slip, porosity medium

ABSTRACT

The present article highlights the impact of variable fluid property for MHD viscous fluid flow containing gyrotactic microorganisms over a permeable stretching sheet. It also considers the variable Prandtl number, variable Schmidt number of mass, variable Schmidt number of gyrotactic microorganisms. It also examined the first and second order velocity slip, temperature jump, concentration slip, microorganism slip, porosity medium, non-liner radiation and non-linear chemical reaction. By using suitable transformation, the governing PDEs corresponding to the momentum, energy, mass and microorganism equations are converted into non-linear coupled ODEs and solved numerically by using R-K 4th order with shooting technique. The effects of physical parameters on the velocity, heat, mass and microorganism are analyzed with the help of graphs and tables.

1. INTRODUCTION

The term bio-convection refers to a macroscopic convection motion of fluid which is caused by the density gradient created by collective swimming of motile microorganisms. These self-propelled motile microorganisms increase the density of the base fluid by swimming in a particular direction, thus causing bio-convection. The concept of nano-fluid bio-convection was introduced by several researchers [1-21]. One of the nice researches on fluid flow over stretching sheet is carried out by Khan and Pop [22]. Nadeem et al. [23] have investigated the radiative slip flow on MHD nanofluid over a stretching sheet. All these researchers considered the flow by taking nanofluids and concluded that motion due to self-propelled microorganisms result in enhancement in mixing and thus preventing nanoparticle cluster.

Heat transfer is a key process throughout a number of residential, industrial, research, engineering and commercial facilities. At all these locations, heat must efficiently and effectively be added, removed or transferred from one process to another to keep the status quo. Also, heat transfer takes place due to many causes. That may be viscous dissipation (frictional heat), non-uniform heat source/sink (internal heat generation/absorption), etc. Further, this model was extensively used by many researchers [24-33] to construct the energy equation and they also discussed the flow and heat transfer behavior of various kinds of Newtonian and non-Newtonian fluids.

The major objective of the present work is to analyse the impact of variable fluid property for MHD viscous fluid flow containing gyrotactic microorganisms over a permeable stretching sheet through porosity medium, non-liner radiation and non-linear chemical reaction. Sheikholeslami et al. [34-35] has studied nanofluid transportation through a permeable media with magnetic force and radiation. Sajjadi et al. [36-37] have proposed the effects of 3-D MHD natural convection on fluid flow and heat transfer. Application of full-spectrum k-distribution method to combined non-gray radiation and forced convection flow in a duct with an expansion was studied by Atashhafrooz et al. [38]. Megahed [47] investigated second order slip velocity and thermal slip effects on MHD viscous Casson fluid flow and heat tranfer. Alama [48] studied the effects of variable fluid properties on unsteady convective boundary flow. Micropolor fluid flow along a non-linear stretching sheet has been studied by Rahmanet al. [49]. Rahman and Eltayeb [50] investigated convective slip flow of rarefied fluids over a wedge with thermal jump and variable transport properties.

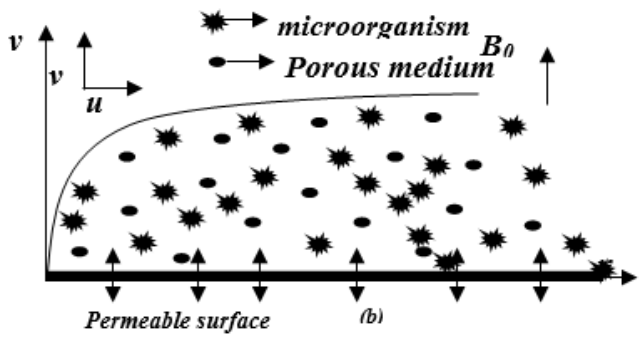

Figure 1. Physical model of the problem

We have considered the variable Prandtl number, variable Schmidt number of mass, variable Schmidt number of gyrotactic microorganisms in temperature, mass and microorganisms profiles and first and second order velocity slip, temperature jump, concentration slip, microorganism slip in boundary conditions. R-K 4th method is applied to solve the transformed boundary layer equations of the flow, heat, mass and microorganisms profiles. Further, the

influence of pertinent parameters such as magnetic field parameter, thermal Grashof number, mass Grashof number, variable Prandtl number, variable Schmidt number of mass, variable Schmidt number of gyrotactic microorganisms, velocity slip, temperature jump, concentration slip, microorganism slip, temperature difference parameter, on velocity, temperature and concentration fields along with friction factor and Nusselt number are examined and shown in graphs and tables. Finally, a comparison of the current work with the earlier results Nadeem and Hussain [39], Gorla and Sidawi [40], Goyal and Bhargava [41], Andersson et al. [42], Prasad et al. [43], Mukhopadhyay et al. [44], Palani et al. [45] and Gorla et al. [46] is also made for the purpose of validating the results.

2. MATHEMATICAL FORMULATION

MHD viscous fluid containing gyrotactic microorganisms flow over a permeable stretching surface in the presence of a magnetic field. A uniform magnetic field is applied at perpendicular to the fluid flow. Joule heating, viscous dissipation and Hall effect are neglected. Hence the Lorentz force depends only on magnetic field. Surface is stretching $u_w = Bx$ along the *x* axis. B is the positive constant.

The continuity, momentum, energy, mass and microorganism equations are given by Waqas et al. [1-2] and Naseem et al. [3]

$$\frac{\partial u}{\partial x}+\frac{\partial v}{\partial y}=0 \tag{1}$$

$$u\frac{\partial u}{\partial x}+v\frac{\partial u}{\partial y}=\frac{1}{\rho_\infty}\frac{\partial}{\partial y}\left(\mu(\mathrm{T})\frac{\partial u}{\partial y}\right)-\left(\frac{\sigma B_0^2}{\rho_\infty}+\frac{\mu(\mathrm{T})}{\rho_\infty k_p}\right)u \tag{2}$$

$$u\frac{\partial T}{\partial x}+v\frac{\partial T}{\partial y}=\frac{1}{\rho_\infty C_p}\frac{\partial}{\partial y}\left(k(\mathrm{T})\frac{\partial T}{\partial y}\right)-\frac{1}{\rho_\infty C_p}\frac{\partial q_r}{\partial y} \tag{3}$$

$$u\frac{\partial C}{\partial x}+v\frac{\partial C}{\partial y}=D_m\frac{\partial^2 C}{\partial y^2}-k_n(C-C_\infty)^n \tag{4}$$

$$u\frac{\partial N}{\partial x}+v\frac{\partial N}{\partial y}+\frac{b_c w_c}{(\mathrm{C}_w-\mathrm{C}_\infty)}\frac{\partial}{\partial y}\left(N\frac{\partial C}{\partial y}\right)=D_n\frac{\partial^2 N}{\partial y^2} \tag{5}$$

where, $u(x,y)$ and $v(x,y)$ are the horizontal and vertical fluid velocity components. T and T_∞ are temperature and ambient fluid temperature. $\mu(\mathrm{T})=\mu_\infty(1+\mathrm{a}(\mathrm{T}-\mathrm{T}_w))$: temperature-dependent viscosity, μ_∞ : ambient viscosity, $k(\mathrm{T})=k_\infty(1+b(\mathrm{T}-\mathrm{T}_\infty))$: temperature dependent thermal conductivity, k_∞ : ambient thermal conductivity, $\varepsilon=b(\mathrm{T}_w-\mathrm{T}_\infty)$: thermal conductivity variation parameter, $\delta=a(\mathrm{T}_w-\mathrm{T}_\infty)$: viscosity variation parameter,

Boundary Conditions [46-47]

$$u=u_w+L_1\frac{\partial u}{\partial y}+L_2\frac{\partial^2 u}{\partial y^2},\ v=-v_w,\ T=T_w+L_3\frac{\partial T}{\partial y},$$
$$C=C_w+L_4\frac{\partial C}{\partial y},N=N_w+L_5\frac{\partial N}{\partial y}\ at\ y=0$$

$$u\to 0,\ T\to T_\infty,\ C\to C_\infty,N\to N_\infty \qquad at\ y\to\infty \tag{6}$$

v_w suction/injection velocity. Following Rosseland approximation q_r , the radiation heat flux is given

$$q_r=-\left(\frac{4\sigma}{3k^*}\right)\frac{\partial T^4}{\partial y}=-\left(\frac{16\sigma}{3k^*}\right)T^3\frac{\partial T}{\partial y}.$$

Solution

We now introduce the following relations for u,v as

$$u=Bxf'(\eta),\ v=-\sqrt{Bv_\infty}\,f(\eta),\eta=y\sqrt{\frac{B}{v_\infty}},\ \theta(\eta)=\frac{T-T_\infty}{T_w-T_\infty},$$
$$\phi=\frac{C-C_\infty}{C_w-C_\infty}\ \text{and}\ \mathrm{N}(\eta)=\frac{N-N_\infty}{N_w-N_\infty} \tag{7}$$

Eqns. (2-6) and using Eq. (7) thus reduces to the following non-dimensional form

$$\begin{aligned}&\left(f'''(1+\delta(1-\theta))-\delta\theta' f''\right)-f'^2+f''f\\&-\left[M+K_p\left(1+\delta(1-\theta)\right)\right]f'=0\end{aligned} \tag{8}$$

$$\begin{aligned}&\theta''\left(1+\frac{4}{3}R\left((\theta_w-1)\theta+1\right)^3+\varepsilon\theta\right)+\varepsilon\theta'^2+\\&4R(\theta_w-1)\theta'^2\left((\theta_w-1)\theta+1\right)^2+\mathrm{Pr}_\infty\left(f\theta'\right)=0\end{aligned} \tag{9}$$

$$\phi''-Sc_\infty\left(K_n\phi^n-f\phi'\right)=0 \tag{10}$$

$$\omega''+Sn_\infty\left(f\omega'-\mathrm{Pe}\left(\omega'\phi'+\phi''(\omega+\sigma)\right)\right)=0 \tag{11}$$

Variable Prandtl number, Variable Schmidt number of mass and Variable Schmidt number of gyrotactic microorganisms

Prandtl number is a function of viscosity, thermal conductivity and specific heat. Viscosity and thermal conductivity are the function of temperature, the Prandtl number also varies. Therefore, the Prandtl number related to the variable viscosity and variable thermal conductivity is defined as

$$\mathrm{Pr}_v=\frac{\mu(\mathrm{T})\mathrm{C}_p}{k(\mathrm{T})}=\frac{\mathrm{C}_p\,\mu_\infty(1+\delta(1-\theta))}{k_\infty(1+\varepsilon\theta)}=\frac{\mathrm{Pr}_\infty(1+\delta(1-\theta))}{(1+\varepsilon\theta)}$$

At the surface η =0 of the porous stretching, this can be written as

$$\mathrm{Pr}_w=\frac{\mathrm{Pr}_\infty(1+\delta)}{(1+\varepsilon)}$$

It can be seen that for δ =0, ε =0 the variable Prandtl number Pr_w is equal to the ambient Prandtl number Pr_∞ . It is mention that $\eta\to\infty$, i.e. outside the boundary-layer, $\theta(\eta)$ becomes zero, therefore, $\mathrm{Pr}_\infty=\mathrm{Pr}_v$ regardless of the values of δ and ε .Schmidt numberis the ratio of viscous diffusivity to

mass diffusivity. If the viscosity of the fluid varies with the temperature, then the Schmidt number varies too. The assumption of constant Schmidt number inside the boundary layer may produce unrealistic results [40-42]. Therefore, the Schmidt number related to the variable viscosity is defined as

$$Sc_v = \frac{\mu(\mathrm{T})}{D_m \rho_\infty} = \frac{\mu_\infty(1+\delta(1-\theta))}{D_m \rho_\infty} = Sc_\infty(1+\delta(1-\theta))$$
$$Sc_N = \frac{\mu(\mathrm{T})}{D_N \rho_\infty} = \frac{\mu_\infty(1+\delta(1-\theta))}{D_N \rho_\infty} = Sc_{N\infty}(1+\delta(1-\theta))$$

At the surface $\eta = 0$ of the porous stretching, this can be written as

$$Sc_v = \frac{\mu(\mathrm{T})}{D_m \rho_\infty} = \frac{\mu_\infty(1+\delta)}{D_m \rho_\infty} = Sc_\infty(1+\delta)$$
$$Sc_N = \frac{\mu(\mathrm{T})}{D_N \rho_\infty} = \frac{\mu_\infty(1+\delta)}{D_N \rho_\infty} = Sc_{N\infty}(1+\delta)$$

It can be seen that for $\delta = 0, \varepsilon = 0$ the variable Prandtl number Sc_w, Sc_{wN} is equal to the ambient Schmidt number of mass and gyrotactic microorganisms $Sc_\infty, Sc_{\infty N}$. It is mention that $\eta \to \infty$, i.e. outside the boundary-layer, $\theta(\eta)$ becomes zero, therefore, $Sc_\infty, Sc_{\infty N} = Sc_v, Sc_{vN}$ regardless of the values of δ and ε.

The non-dimensional temperature Eqns. (8-11) can be expressed as

$$\begin{aligned}&\theta''\left(1+\frac{4}{3}R\left((\theta_w-1)\theta+1\right)^3+\varepsilon\theta\right)+\varepsilon\theta'^2\\&+4R(\theta_w-1)\theta'^2\left((\theta_w-1)\theta+1\right)^2\\&+\frac{\mathrm{Pr}_v(1+\varepsilon\theta)}{(1+\delta(1-\theta))}\left(f\theta'\right)=0\end{aligned} \tag{12}$$

$$\phi''-\frac{Sc_v}{(1+\delta(1-\theta))}\left(K_n\phi^n - f\phi'\right)=0 \tag{13}$$

$$\begin{aligned}&\omega''+\frac{Sn_v}{(1+\delta(1-\theta))}\\&\left(f\omega'-\mathrm{Pe}\left(\omega'\phi'+\phi''(\omega+\sigma)\right)\right)=0\end{aligned} \tag{14}$$

Boundary conditions equations (6) reduces as:

$$\begin{aligned}&\eta=0: \quad f'(\eta)=1+Slip_1 f''(\eta)+Slip_2\, f'''(\eta),\\&f(\eta)=S,\ \theta(\eta)=1+Slip_T\theta'(\eta),\\&\phi(\eta)=1+Slip_C\phi'(\eta),\quad \omega(\eta)=1+Slip_C\omega'(\eta)\\&\eta\to\infty: \quad f'(\eta)\to 0,\ \theta(\eta)\to 0,\phi(\eta)\to 0,\\&\omega(\eta)\to 0\end{aligned} \tag{15}$$

where, $Slip_1 = L_1\sqrt{\frac{B}{\nu_\infty}}$; $Slip_2 = L_2\frac{B}{\nu_\infty}$ $Slip_T = L_3\sqrt{\frac{B}{\nu_\infty}}$, $Slip_C = L_4\sqrt{\frac{B}{\nu_\infty}}$, $Slip_N = L_5\sqrt{\frac{B}{\nu_\infty}}$: first and second order slip velocity parameter, slip temperature parameter, slip concentration parameter and slip microorganism parameter respectively, $R = \frac{4\sigma T_\infty^3}{k_\infty k^*}$; Radiation parameter, k^*; thermal radiation parameter, $M = \frac{\sigma B_0^2}{\rho_\infty B}$: Magnetic field parameter, $K_n = \frac{k_n}{b}(C_w - C_\infty)^{n-1}$: chemical reaction parameter, $\theta_w = \frac{T_w}{T_\infty}$: temperature difference parameter, k_∞: thermal conductivity $K_p = \frac{\nu_\infty}{k_p b}$: porosity parameter, $Pe = \frac{b_c w_c}{\nu_\infty}$: bioconvection Péclet number, $\sigma = \frac{N_\infty}{N_w - N_\infty}$:bioconvection constant, $Sn_\infty = \frac{\nu_\infty}{D_n}$: ambient Schmidt number of microorganism, $Sc_\infty = \frac{\nu_\infty}{D_B}$: ambient Schmidt number of mass $\mathrm{Pr}_\infty = \frac{\mu_\infty}{k_\infty}C_p$ ambient Prandtl number.

3. RESULTS AND DISCUSSION

In this article, the influence of various physical parameters like magnetic field parameter, first and second order slip velocity parameter, slip temperature parameter, slip concentration parameter and slip microorganism parameter radiation parameter, chemical reaction parameter, temperature difference parameter, porosity parameter, bioconvection Péclet number, bioconvection constant, ambient Schmidt number of microorganism, ambient Schmidt number of mass, ambient Prandtl number is examined. These values are kept as common in entire study except the varied values as shown in respective figures and tables. Figures 2-5 the f, θ, ϕ and ω profiles are plotted for the (M) and other parameters are kept fixed. The f of fluid increase as (M) increases and the θ, ϕ and ω flux decrease as the value of (M) increase. This is due to the fact that the magnetic field introduces a retarding body force known as Lorentz force. As the Lorentz force is a resistive force which opposes the fluid motion, so heat is produced and as a result, the thermal boundary layer thickness and concentration (volume fraction) boundary layer thickness become thicker for stronger magnetic field. Physically, the drag force increases with an increase in the magnetic field and as a result depreciation occurs in the velocity field.

Figures 6-9 depicts the f, θ and ϕ profiles are plotted for the (k_p) and other parameters are kept fixed. The f of fluid decreases as (k_p) increases and the θ, ϕ and ω flux increase as the value of (k_p) increases. Figures 10-17 show the impact of ($slip_1$ & $slip_2$)parameter on f, θ, ϕ and ω profiles. It is observed that for increasing values of ($slip_1$ & $slip_2$) parameter, the f decrease whereas θ, ϕ and ω profiles increase. Figure 18 shows the impact of ($slip_T$) parameter on θ profile. It is observed that for increasing values of ($slip_T$), the θ profile decrease. Figures 19-20 show the impact of (

$slip_c$) parameter on ϕ and ω profiles. It is observed that for increasing values of ($slip_c$), the ϕ and ω profiles decrease. Physically, when slip occurs, the slipping fluid shows a decrease in the surface skin-friction between the fluid and the surface, because not all the pulling force of the surface can be transmitted to the fluid. So, increasing the value of the velocity slip parameter will decrease the flow velocity in the region of the boundary layer. Figure 21 shows the impact of ($slip_2$) parameter on θ profile. It is observed that for increasing values of ($slip_2$), the θ profile decrease. Figures 22-23 show that the heat of the fluid enhances with the increase of (R), (θ_w). Generally, an increment in (R) causes a decrease in absorption coefficient, which results rise in the divergence of radiative heat flux. Hence, the rate of radiative heat transfers of the fluid shoots up, so that the heat flux increases. Figure 24 shows the mass profile is plotted for the (n) other parameters are kept fixed. Concentration of fluid increases as (n) increase. Figure 25 depicts that the temperature profile for the several values of the (Pr) and other parameters are kept fixed. Heat of fluid decreases as (Pr) increases. Prandtl number is used to increase the rate of cooling in conducting flow. At high Prandtl number the fluid is very viscous and the viscous dissipation produces heat due to drag between the fluid particles and this extra heat causes an increase of the initial fluid temperature. Figure 26 shows the ω profile is plotted for the (Sn_v) other parameters are kept fixed. The ω profile of fluid decreases as (Sn_v) increase. Figure 27 depicts that the concentration of the fluid suppresses with the rise the value of (K_n). Physically, chemical reaction increases the rate of interfacial mass transfer. Chemical reaction suppresses the local concentration and increases its mass gradient and its flux. It is due to the fact that (Sc_v) is the ratio of velocity to mass diffusivities which means when (Sc_v) increases, mass diffusivity decreases and there is a reduction in mass. Figures 28-30 show the ω profile against the similarity variable η for various values of following parameters such as Pé, σ and $slip_N$. We are noted that the ω profile decreases Pé, σ and $slip_N$ increases. Figures 31-32 show the impact of (Sc_v) parameter on ϕ and ω profiles. It is observed that for increasing values of (Sc_v) parameter parameter, the ϕ and ω profiles. Table 1 and 2 shows the comparison of the present results with the existed results of Nadeem and Hussain [39], Gorla and Sidawi [40], Goyal and Bhargava [41], Andersson et al. [42], Prasad et al. [43], Mukhopadhyay et al. [44], Palani et al. [45] and Gorla et al. [46]. Under some special conditions, present results have an excellent agreement with the existed results. This shows the validity of the present results along with the accuracy of the numerical technique used in this study. Table 3-4 shows that the variation of skin friction coefficient, local Nusselt number, local Sherwood number and local gyrotactic microorganisms Sherwood number for various physical parameters.

Table 1. Comparison of $-\theta'(0)$ for different values Pr in the absence of the parameters S= M=R=Kp=We= $slip_1$ = $slip_2$ = $slip_T$ = ε = δ =0.0; θ_w =1

Pr	HAM method Nadeem and Hussain [39]	Gorla and Sidawi [41]	FEM method Goyal andBhargava [42]	RKF45 method Gorla et al. [47]	R-K 4th order present study
0.2	0.169	0.1691	0.1691	0.170259788	0.172348764
0.7	0.454	0.5349	0.4539	0.454447258	0.453917857
2	0.911	0.9114	0.9113	0.911352755	0.911361492
7	—	1.8905	1.8954	1.895400395	1.895412536
20	—	3.3539	3.3539	3.353901838	3.353933867

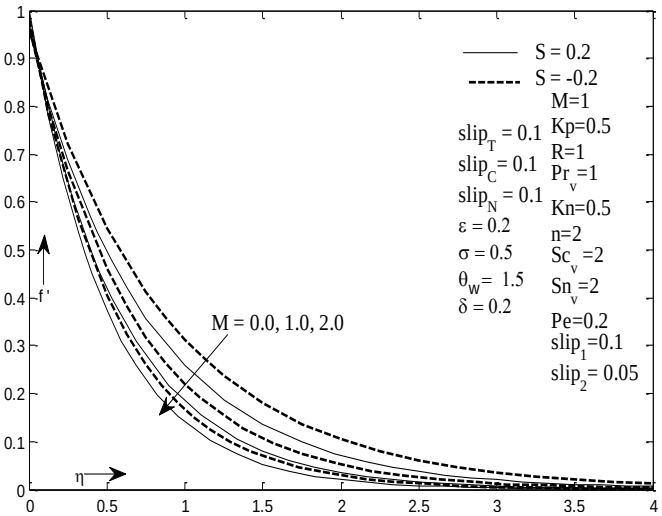

Figure 2. Impact of M on velocity profile

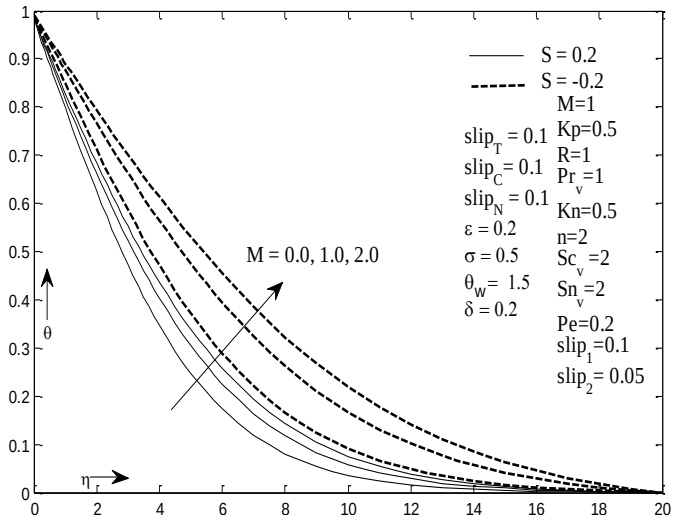

Figure 3. Impact of M on temperature profile

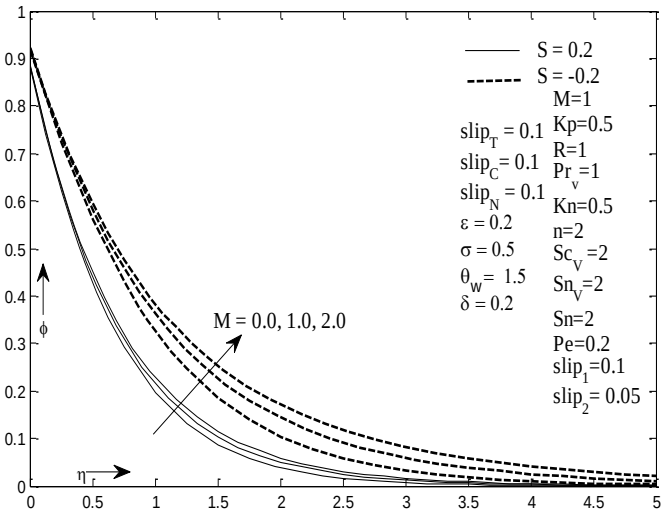

Figure 4. Impact of *M* on mass profile

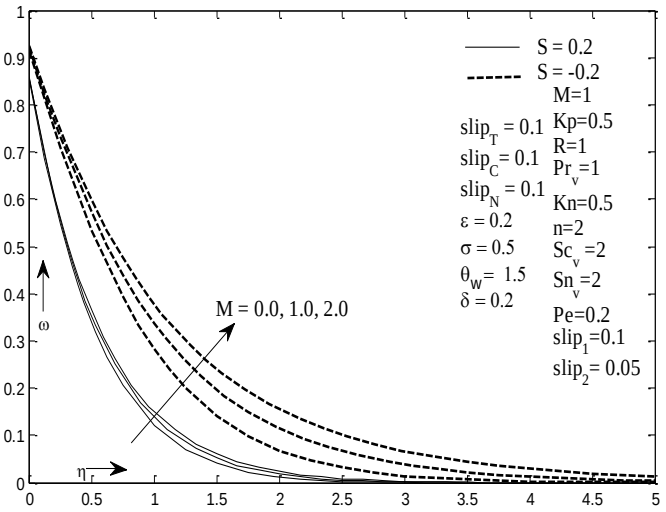

Figure 5. Impact of *M* on microorganism profile

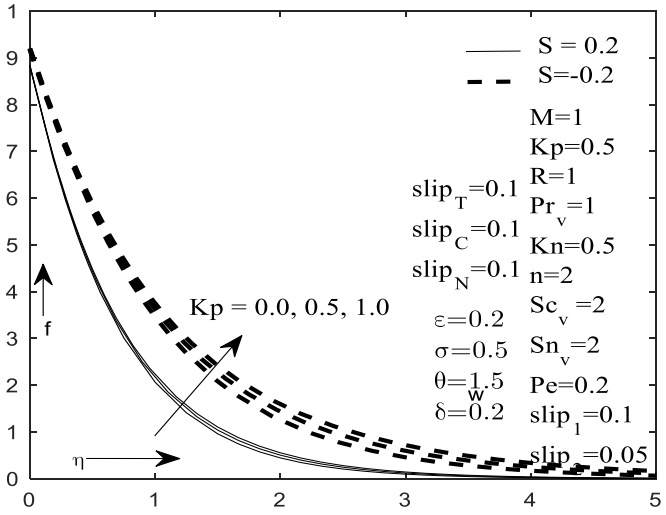

Figure 6. Impact of k_p on velocity profile

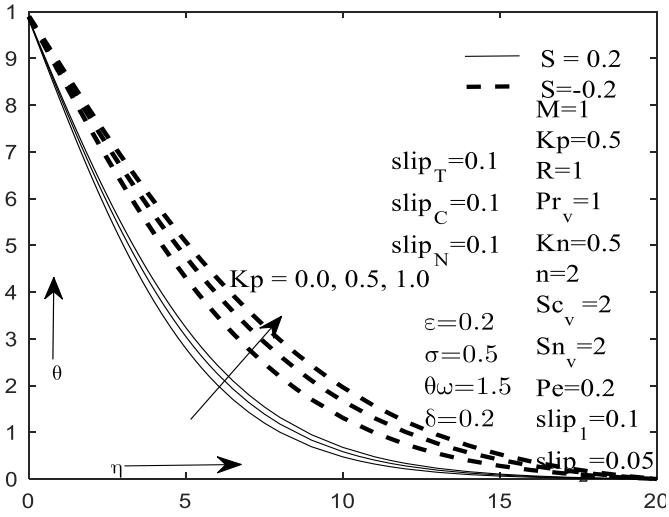

Figure 7. Impact of k_p on temperature profile

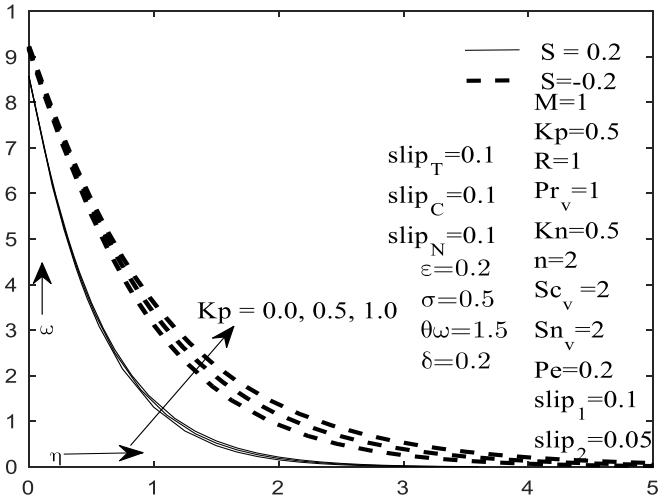

Figure 8. Impact of k_p on mass profile

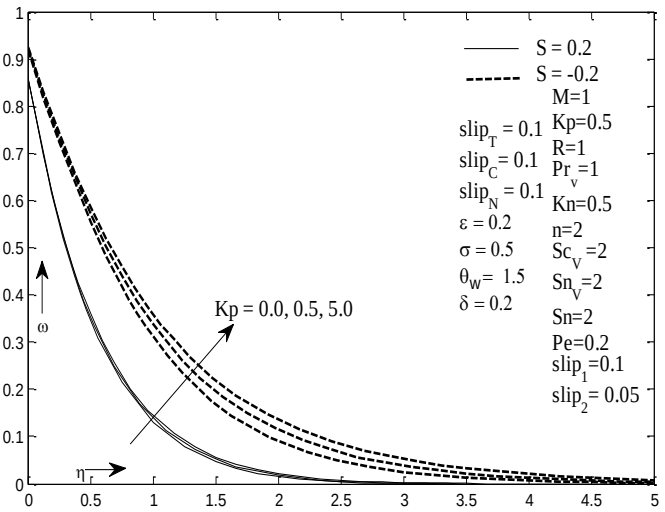

Figure 9. Impact of k_p on microorganism profile

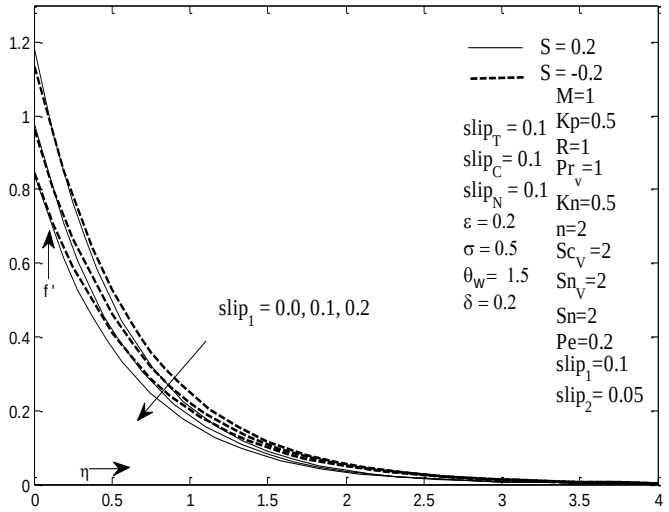

Figure 10. Impact of $slip_1$ on velocity profile

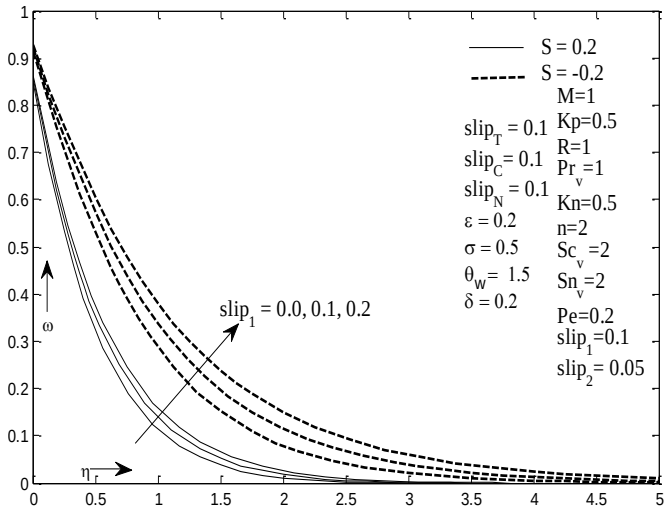

Figure 13. Impact of $slip_1$ on microorganism profile

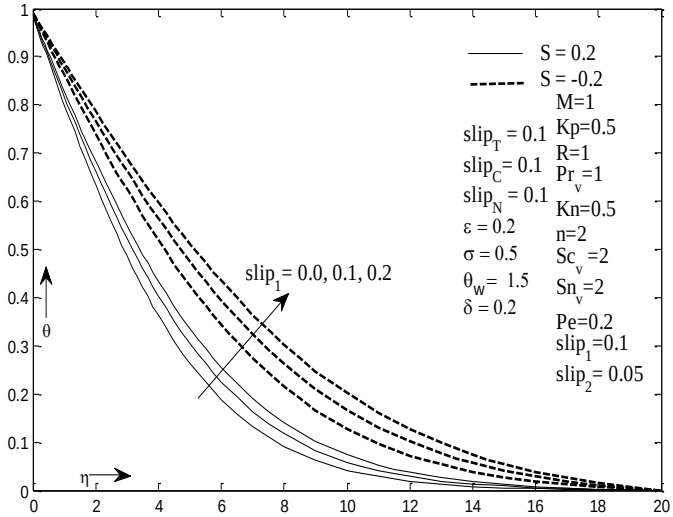

Figure 11. Impact of $slip_1$ on temperature profile

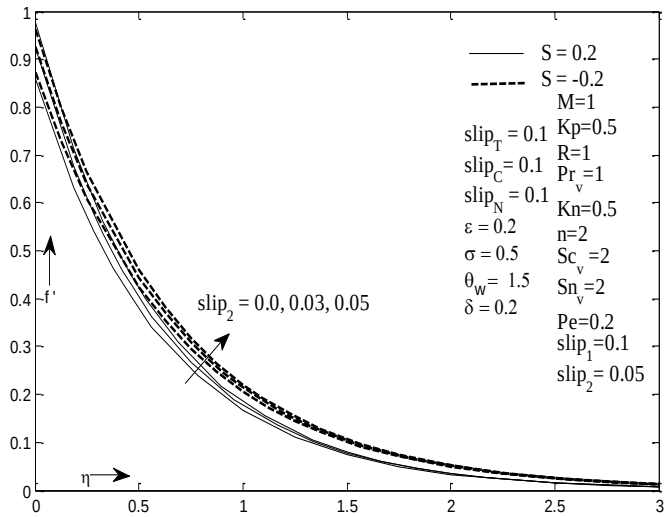

Figure 14. Impact of $slip_2$ on velocity profile

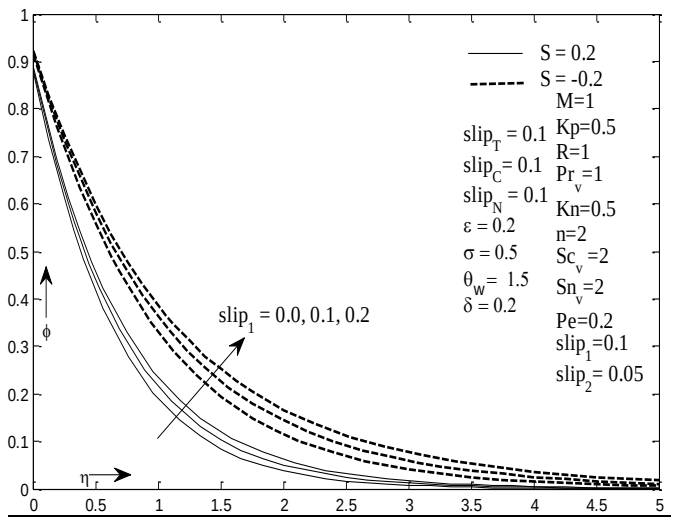

Figure 12. Impact of $slip_1$ on mass profile

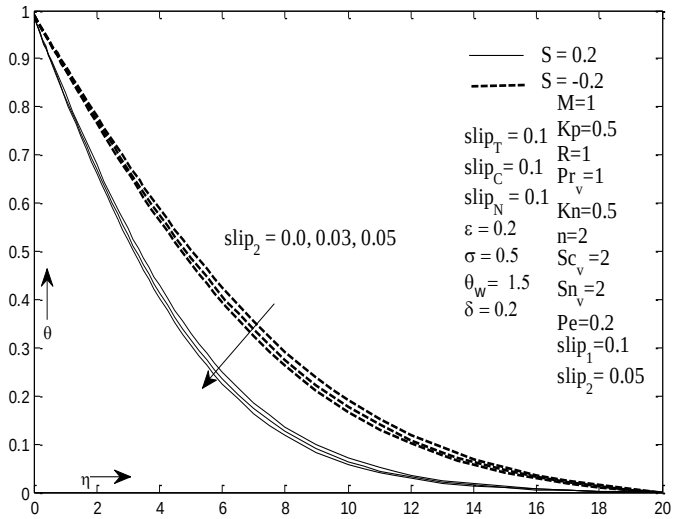

Figure 15. Impact of $slip_2$ on temperature profile

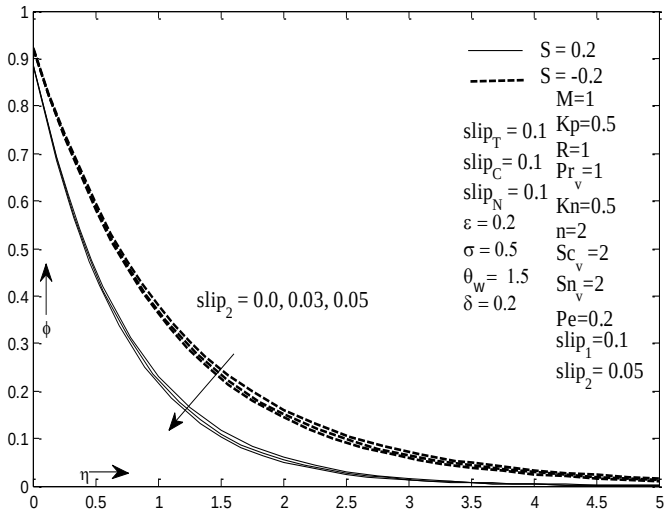

Figure 16. Impact of $slip_2$ on mass

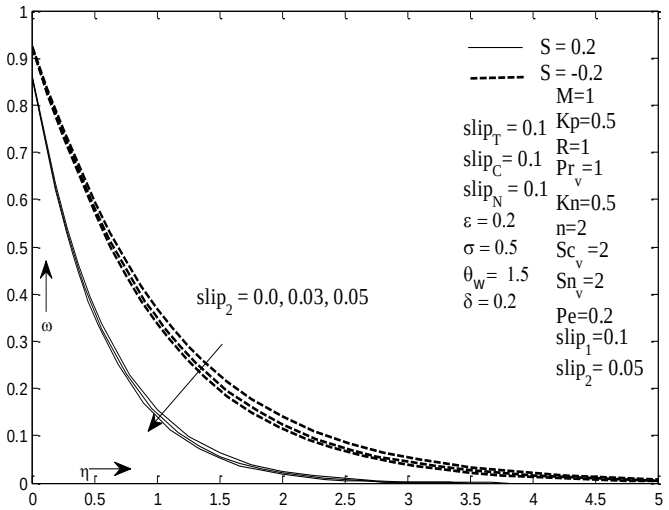

Figure 17. Impact of $slip_2$ on microorganism profile

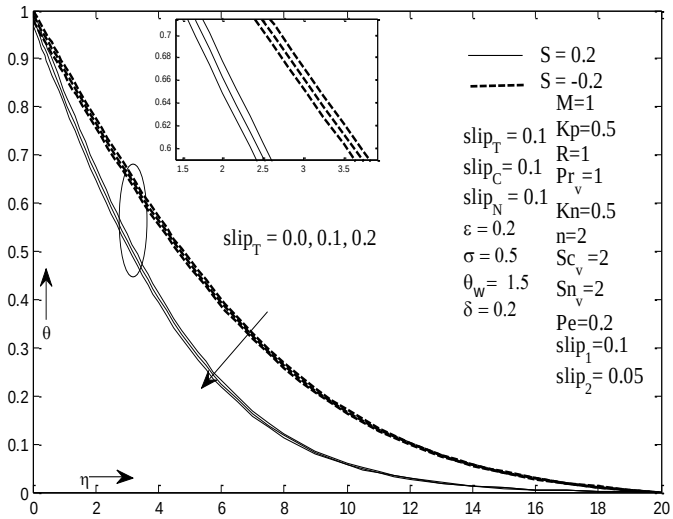

Figure 18. Impact of $slip_T$ on temperature profile

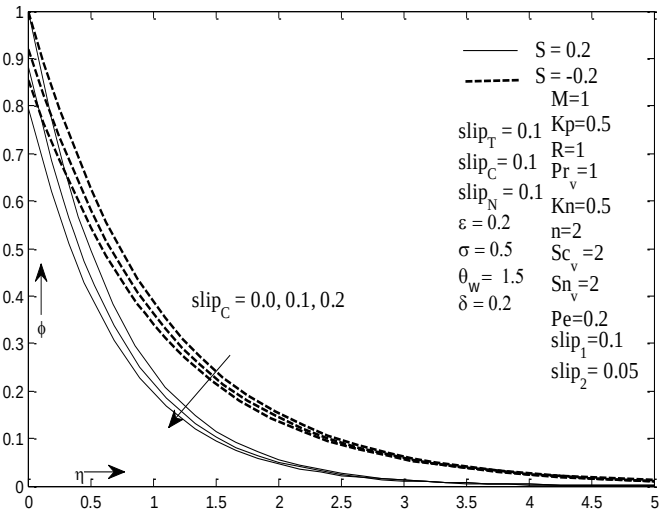

Figure 19. Impact of $slip_C$ on mass profile

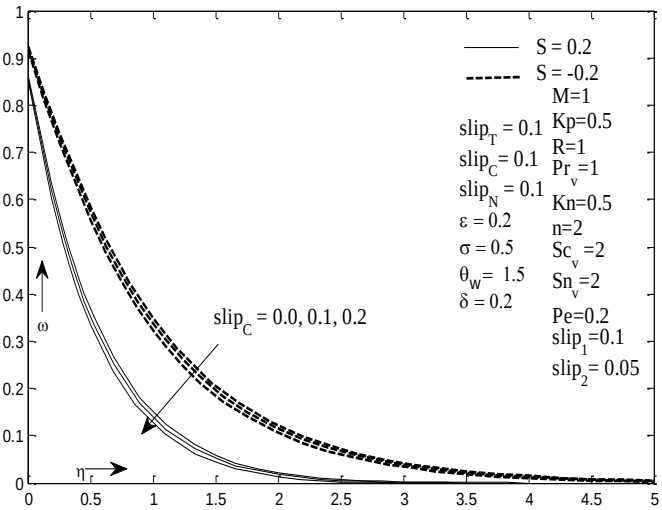

Figure 20. Impact of $slip_C$ on microorganism profile

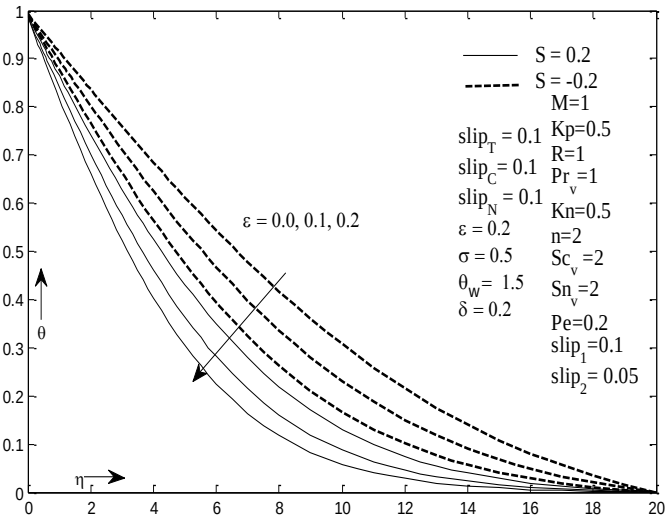

Figure 21. Impact of ε temperature profile

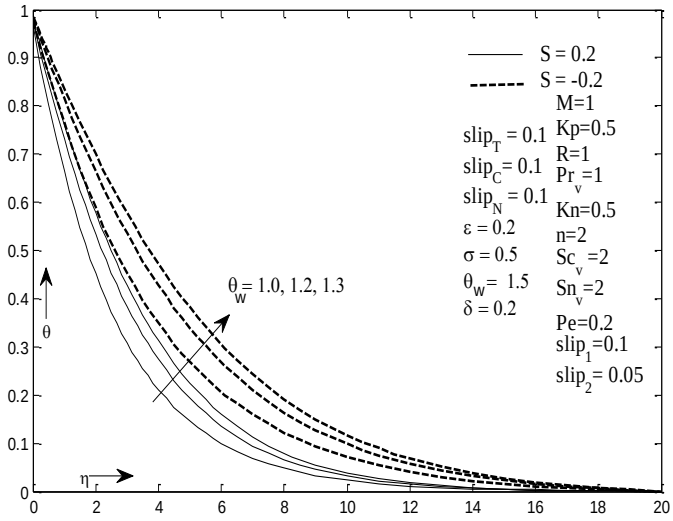

Figure 22. Impact of θ_w on temperature profile

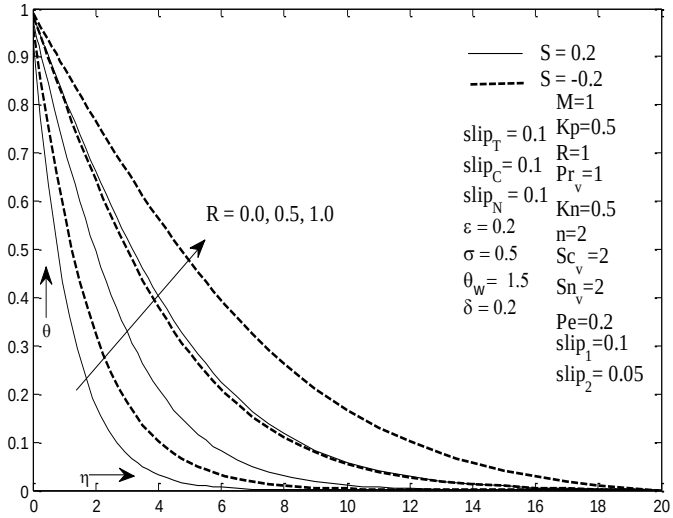

Figure 23. Impact of R on temperature profile

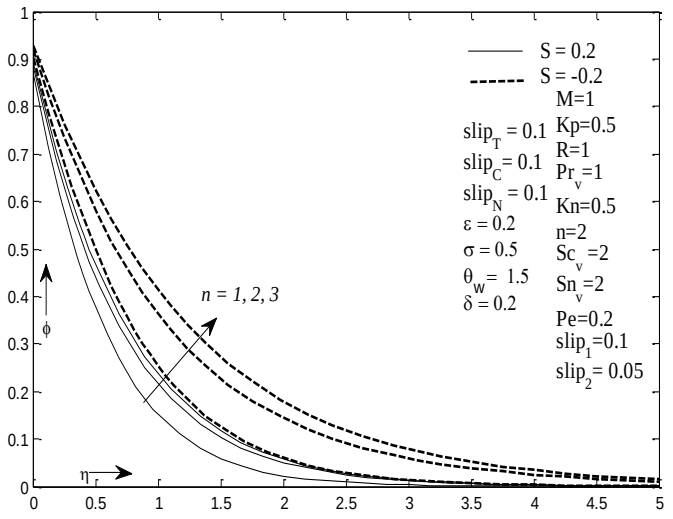

Figure 24. Impact of *n* on mass profile

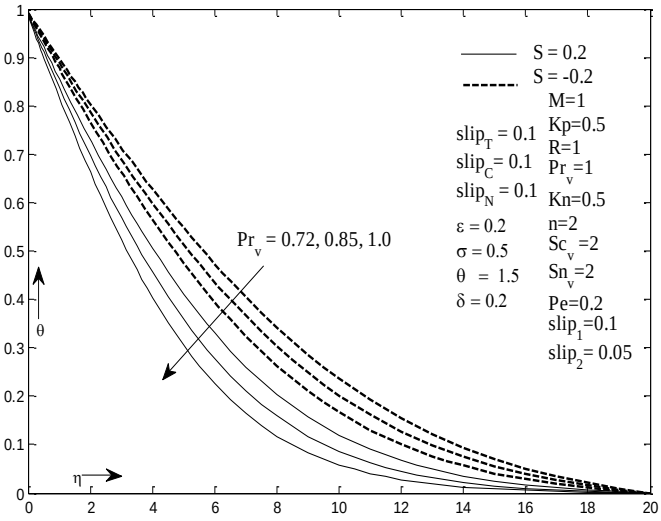

Figure 25. Impact of Pr_v on temperature profile

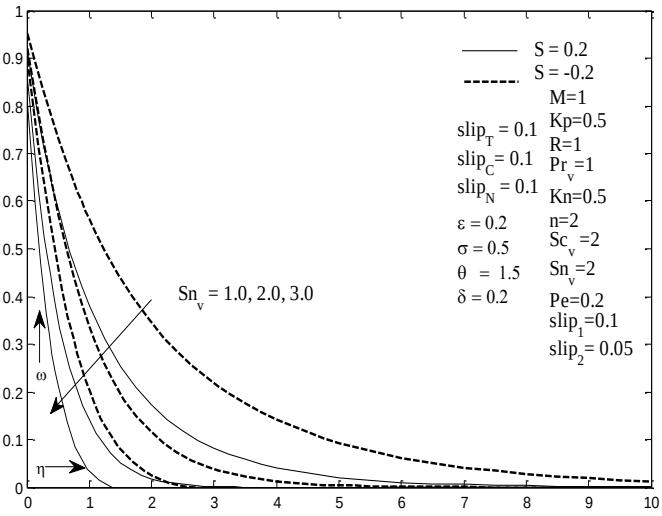

Figure 26. Impact of Sn_v on microorganism profile

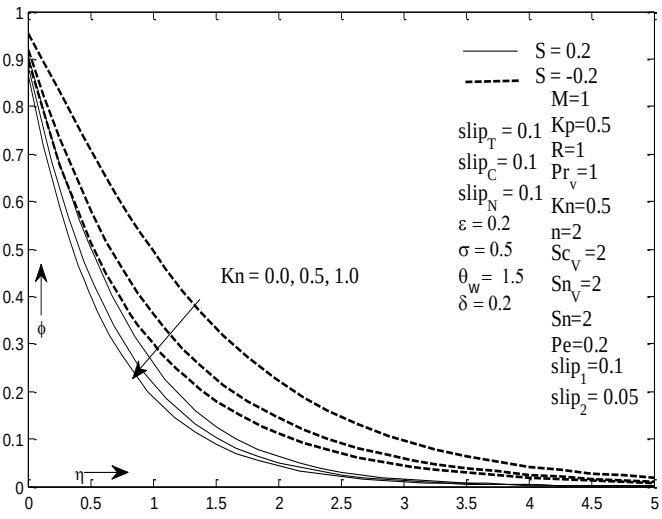

Figure 27. Impact of Kn on mass profile

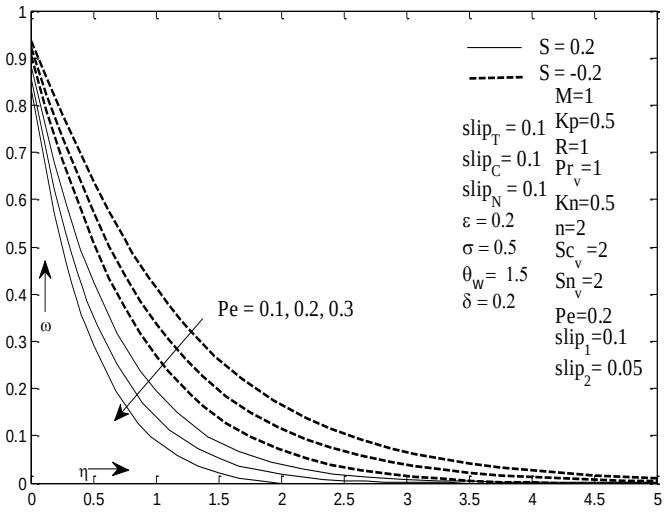

Figure 28. Impact of Pe on microorganism profile

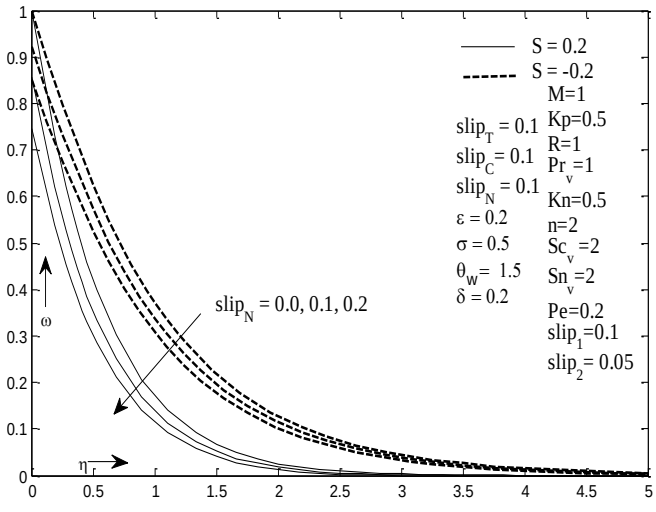

Figure 30. Impact of $slip_N$ on concentration profile

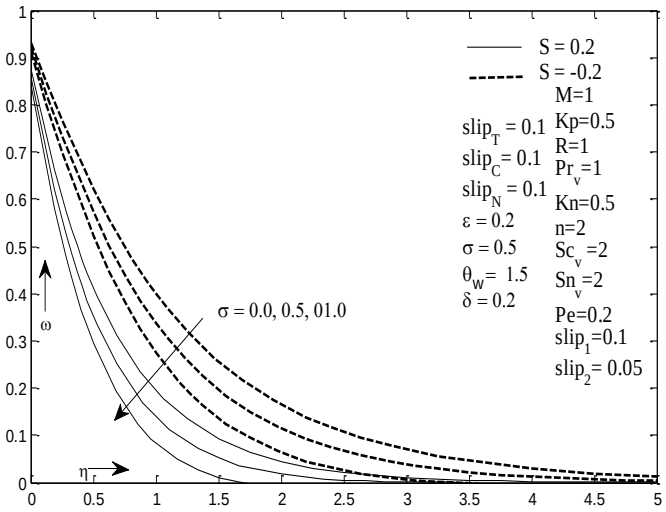

Figure 29. Impact of σ on microorganism profile

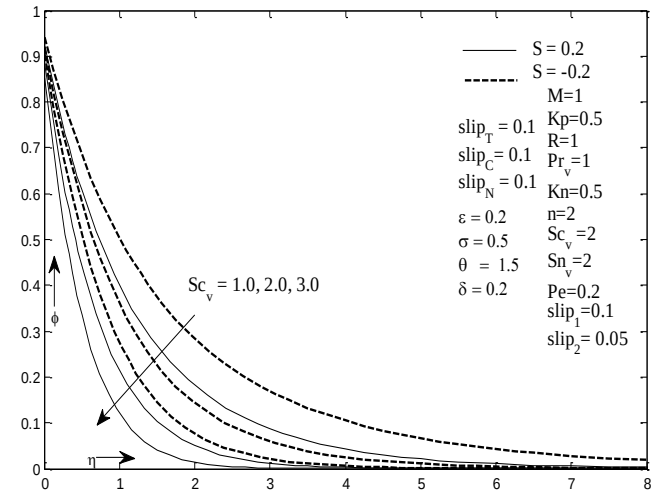

Figure 31. Impact of Sc_v on concentration profile

Table 2. Comparison of $-f''(0)$ for different values M in the absence of the parameters S= R=Kp= $We = slip_1 = slip_2 = slip_T = \varepsilon = \delta = 0.0$; $\theta_w = 1$, Pr=0.72

M	Andersson et al. [42]	Prasad et al. [43]	Mukhopadhyay et al. [44]	Palani et al. [45]	Present study
0.0	1.000000	1.000174	1.000173	1.00000	1.000000000
0.5	1.224900	1.224753	1.224753	1.224745	1.224744871
1	1.414000	1.414449	1.414450	1.414214	1.414213562
1.5	1.581000	1.581139	1.581140	1.581139	1.581138830
2	1.732000	1.732203	1.732203	1.732051	1.732050808

Table 3. Variation of local Nusselt number, local Sherwood number and local gyrotactic microorganisms Sherwood number for various physical parameters

ε	R	θ_w	n	Pr_v	Sn	Kn	Pe	σ	$slip_N$	$-\theta'(0)$	$-\phi'(0)$	$--\omega'(0)$
0.2										0.675182220		
0.4										0.791666927		
0.6										0.907057220		
	0.0									0.672452398		
	0.5									0.857743356		
	1.0									0.907057220		
		1								0.804888907		
		1.2								0.853297614		
		1.3								0.873799158		

			1								1.321873369	
			2								1.165526785	
			3								1.093296359	
				0.72						0.715699806		
				0.85						0.808371394		
				1.0						0.907057220		
					1.5							1.148806504
					2							1.428303592
					2.5							1.680515788
						0.0					0.945201672	
						0.5					1.165526785	
						1.0					1.332019354	
							0.1					1.189603361
							0.2					1.428303592
							0.3					1.661265580
								0.0				1.262732944
								0.5				1.428303592
								1.0				1.593874604
									0.0			1.634725755
									0.1			1.428303592
									0.2			1.268167888

Table 4. Variation of skin friction coefficient, local Nusselt number, local Sherwood number and local gyrotactic microorganisms Sherwood number for various physical parameters

M	Kp	$slip_1$	$slip_2$	$slip_T$	$slip_C$	$f''(0)$	$-\theta'(0)$	$-\phi'(0)$	$--\omega'(0)$
0						-1.265354	1.004250	1.191662	1.464307
1						-1.641575	0.907057	1.165526	1.428303
2						-1.977595	0.852901	1.149273	1.405030
	0					-1.458759	0.949793	1.177437	1.444907
	0.5					-1.641575	0.907057	1.165526	1.428303
	1					-1.813989	0.875559	1.156204	1.415042
		0.0				-2.066579	0.988152	1.218744	1.509977
		0.1				-1.641575	0.907057	1.165526	1.428303
		0.2				-1.374705	0.850296	1.128698	1.369648
			0.0			-1.413180	0.858801	1.134191	1.378525
			0.03			-1.539607	0.885967	1.151798	1.406668
			0.05			-1.641575	0.907057	1.165526	1.428303
				0.0			0.912196		
				0.1			0.907057		
				0.2			0.901785		
					0.0			1.351283	
					0.1			1.165526	
					0.2			1.028143	

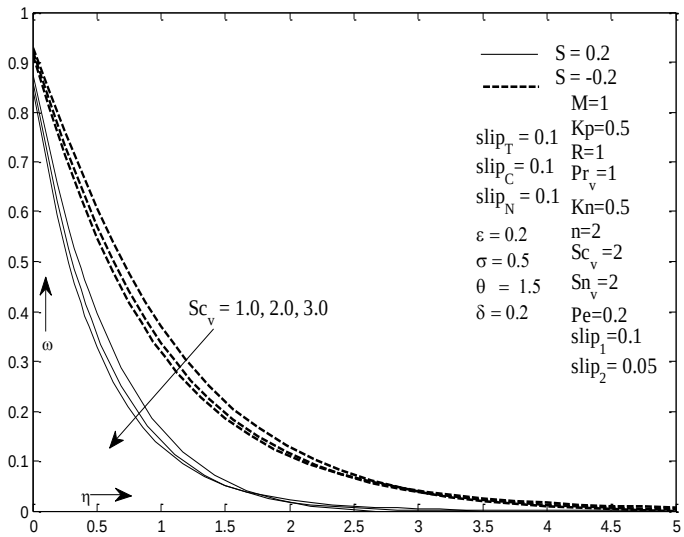

Figure 32. Impact of Sc_v on microorganisms profile

4. CONCLUSION

We have discussed variable fluid property for MHD viscous fluid flow containing gyrotactic microorganisms over a permeable stretching sheet and also considered the variable Prandtl number, variable Schmidt number of mass, variable Schmidt number of gyrotactic microorganisms, first and second order velocity slip, temperature jump, concentration slip, microorganism slip, porosity medium, non-liner radiation and non-linear chemical reaction. By using suitable transformation, the governing PDEs corresponding to the momentum, energy, mass and microorganism equations are converted into non-linear coupled ODEs and numerically by using R-K 4th order with shooting technique. The effects of physical parameters on the velocity, heat, mass and microorganism are analyzed with the help of graphs and tables.

The following important results can be drawn from this study:

- The dimensionless velocity is a decreasing function of (M), (k_p) and ($slip_1$) parameters increases whereas temperature, concentration and microorganism profiles growing.
- The dimensionless velocity is increasing function of ($slip_2$) parameters increases whereas temperature, concentration and microorganism profiles decreasing.
- Inside thermal boundary layer, the dimensionless temperature increases with (R), (θ_w) parameters increase.
- The reduced thermal boundary layer thickness with ($slip_T$), (ε) and (Pr) parameter increases.
- The reduced concentration and microorganism profiles with ($slip_c$) parameter increases.
- (M) parameter is high influence of f'''.
- The reduced microorganism profile with ($slip_N$), (σ), (Sn_v) and (Pe) parameter increases.
- The concentration boundary layer increases with (n) increases and opposite behavior show to increase (K_n) on concentration profile.

REFERENCES

[1] Waqas, M., Hayat, T., Khan, M.I., Alsaedi, A. (2017). Behaviour of stratification phenomenon in flow of Maxwell nanomaterial with motile gyrotactic microorganisms in the presence of magnetic field. International Journal of Mechanical Sciences, (131-132): 426-434. https://doi.org/10.1016/j.ijmecsci.2017.07.009

[2] Waqas, M., Hayat, T., Shehzad, S.A., Alsaedi, A. (2018). Transport of magnetohydrodynamic nanomaterial in a stratified medium considering gyrotactic microorganisms. Physica B: Condensed Matter, 529: 33-40. https://doi.org/10.1016/j.physb.2017.09.128

[3] Naseem, F., Shafiq, A., Zhao, L., Naseem, A. (2017). MHD biconvective flow of Powell Eyring nanofluid over stretched surface. AIP Advances, 7: 065013. https://doi.org/10.1063/1.4983014

[4] Khan, U., Ahmed, N., Mohyud-Din, S.T. (2016). Influence of viscous dissipation and joule heating on MHD bio-convection flow over a porous wedge in the presence of nanoparticles and gyrotactic microorganisms. Springer Plus, 5: 2043. https://doi.org/10.1186/s40064-016-3718-8

[5] Avramenko, A.A., Kuznetsov, A.V. (2004). Stability of a suspension of gyrotactic microorganisms in superimposed fluid and porous layers. International Communications in Heat and Mass Transfer, 31(8): 1057-1066. https://doi.org/10.1016/j.icheatmasstransfer.2004.08.003

[6] Khan, W.A., Makinde, O.D. (2014). MHD nanofluid bioconvection due to gyrotactic microorganisms over a convectively heat stretching sheet. International Journal of Thermal Sciences, 81: 118-124. https://doi.org/10.1016/j.ijthermalsci.2014.03.009

[7] Khan, W.A., Makinde, O.D., Khan, Z.H. (2014). MHD boundary layer flow of a nanofluid containing gyrotactic microorganisms past a vertical plate with Navier slip. International Journal of Heat and Mass Transfer, 74: 285-291. https://doi.org/10.1016/j.ijheatmasstransfer.2014.03.026

[8] Nield, D.A., Kuznetsov, A.V. (2006). The onset of bio-thermal convection in a suspension of gyrotactic microorganisms in a fluid layer: Oscillatory convection. Int. J. Therm. Sci., 45(10): 990-997. https://doi.org/10.1016/j.ijthermalsci.2006.01.007

[9] Kuznetsov, A.V. (2011). Bio-thermal convection induced by two different species of microorganisms. International Communications in Heat and Mass Transfer, 38(5): 548-553. https://doi.org/10.1016/j.icheatmasstransfer.2011.02.006

[10] Kuznetsov, A.V. (2006). The onset of thermo-bioconvection in a shallow fluid saturated porous layer heated from below in a suspension of oxytactic microorganisms. European Journal of Mechanics – B/Fluids, 25(2): 223-233. https://doi.org/10.1016/j.euromechflu.2005.06.003

[11] Hill, N.A., Pedley, T.J. (2005). Bioconvection. Fluid Dynamics Research, 37(1/2): 1-20. https://doi.org/10.1016/j.fluiddyn.2005.03.002

[12] Alloui, Z., Nguyen, T.H., Bilgen, E. (2007). Numerical investigation of thermo-bioconvection in a suspension of gravitactic microorganisms. Int. J. Heat Mass Transfer, 50(7-8): 1435-1441. https://doi.org/10.1016/j.ijheatmasstransfer.2006.09.008

[13] Hillesdon, A.J., Pedley, T.J., Kessler, J.O. (1995). The development of concentration gradients in a suspension of chemotactic bacteria. Bulletin of Mathematical Biology, 57(2): 299-344. https://doi.org/10.1016/0092-8240(94)00038-E

[14] Hillesdon, A.J., Pedley, T.J. (1996). Bioconvection in suspensions of oxytactic bacteria: Linear theory. Journal of Fluid Mechanics, 324: 223-259. https://doi.org/10.1017/S0022112096007902

[15] Childress, S., Levandowsky, M., Spiegel, E.A. (1975). Pattern formation in a suspension of swimming microorganisms – equations and stability theory. Journal of Fluid Mechanics, 69(3): 591-613. https://doi.org/10.1017/S0022112075001577

[16] Pedley, T.J., Hill, N.A., Kessler, J.O. (1988). The growth of bioconvection patterns in a uniform suspension of gyrotactic microorganisms. Journal of Fluid Mechanics, 195: 223-237. https://doi.org/10.1017/S0022112088002393

[17] Hill, N.A., Pedley, T.J., Kessler, J.O. (1989). Growth of bioconvection patterns in a suspension of gyrotactic microorganisms in a layer of finite depth. Journal of Fluid Mechanics, 208: 509-543. https://doi.org/10.1017/S002211208900292

[18] Spormann, A.M. (1987). Unusual swimming behaviour of a magneto tactic bacterium. FEMS Microbiology Ecology, 3(1): 37-45. https://doi.org/10.1111/j.1574-6968.1987.tb02336.x

[19] Kuznetsov, A.V. (2010). The onset of nanofluid bioconvection in a suspension containing both nanoparticles and gyrotactic microorganisms. International Communications in Heat and Mass Transfer, 37(10): 1421-1425. https://doi.org/10.1016/j.icheatmasstransfer.2010.08.015

[20] Kuznetsov, A.V. (2011). Nanofluid bioconvection in water-based suspensions containing nanoparticles and

oxytactic microorganisms: Oscillatory in stability. Nanoscale Res. Lett., 6(1): 100. https://doi.org/10.1186/1556-276X-6-100
[21] Kuznetsov, A.V. (2011). Non-oscillatory and oscillatory nanofluid bio-thermal convection in a horizontal layer of finite depth. European Journal of Mechanics – B/Fluids, 30(2): 156-165. https://doi.org/10.1016/j.euromechflu.2010.10.007
[22] Khan, W.A., Pop, I. (2010). Boundary-layer flow of a nanofluid past a stretching sheet. International Journal of Heat and Mass Transfer, 53(11-12): 2477-83. https://doi.org/10.1016/j.ijheatmasstransfer.2010.01.032
[23] Haq, R.U., Nadeem, S., Khan, Z.H., Akbar, N.S. (2015). Thermal radiation and slip effects on MHD stagnation-point flow of nanofluid over a stretching sheet. Physica E: Low-dimensional Systems and Nanostructures, 65: 17-23. https://doi.org/10.1016/j.physe.2014.07.013
[24] Aziz, A., Khan, W.A., Pop, I. (2012). Free convection boundary layer flow past a horizontal flat plate embedded in porous medium filled by nanofluid containing gyrotactic microorganisms. International Journal of Thermal Sciences, 56: 48-57. https://doi.org/10.1016/j.ijthermalsci.2012.01.011
[25] Yao, S.S., Fang, T.G., Zhong, Y.F. (2011). Heat transfer of a generalized stretching/shrinking wall problem with convective boundary conditions. Communications in Nonlinear Sciences and Numerical Simulation, 16(2): 752-760. https://doi.org/10.1016/j.cnsns.2010.05.028
[26] Makinde, O.D., Aziz, A. (2011). Boundary layer flow of a nano fluid past a stretching sheet with convective boundary conditions. International Journal of Thermal Sciences, 50(7): 1326-1332. https://doi.org/10.1016/j.ijthermalsci.2011.02.019
[27] Ramesh, G.K., Gireesh, B.J. (2014). Influence of heat source/sink on a Maxwell fluid over a stretching surface with convective boundary condition in the presence of nanoparticles. Ain Shams Engineering Journal, 5(3): 991-998. https://doi.org/10.1016/j.asej.2014.04.003
[28] Jain, S., Choudhary, R. (2017). Soret and Dufour effects on MHD fluid flow due to moving permeable cylinder with radiation. Global and Stochastic Anal., SI: 75-84.
[29] Jain, S., Choudhary, R. (2015). Effects of MHD on boundary layer flow in porous medium due to exponentially shrinking sheet with slip. Procedia Engineering, 127: 1203-1210. https://doi.org/10.1016/j.proeng.2015.11.464
[30] Parmar, A. (2017). Unsteady convective boundary layer flow for MHD Williamson fluid over an inclined porous stretching sheet with non-linear radiation and heat source. International Journal of Applied and Computational Mathematics, 3: 859-881. https://doi.org/10.1007/s40819-017-0387-4
[31] Atashafrooz, M., Gandjalikhan Nassab, S.A., Lari, K. (2016). Numerical analysis of interaction between non gray radiation and forced convection flow over a recess using the full spectrum k distribution method. Heat and Mass Transfer, 52(2): 361-377. https://doi.org/10.1007/s00231-015-1561-z
[32] Atashafrooz, M., Gandjalikhan Nassab, S.A., Lari, K. (2016). Coupled thermal radiation and mixed convection step flow of non-Gray gas. Journal of Heat Trans. (ASME), 138(7): 072701. https://doi.org/10.1115/1.4033095
[33] Rahman, M.M. (2012). Combined effects of internal heat generation and higher order chemical reaction on the non-Darcian forced convective flow of a viscous incompressible fluid with variable viscosity and thermal conductivity over a stretching surface embedded in a porous medium. Can. J. Chem. Eng., 90: 1631-44.
[34] Sheikholeslami, M., Sajjadi, H., Amiri Detouei, A., Atashafrooz, M., Li, Z.X. (2018). Magnetic force and radiation influences on nanofluid transportation through a permeable media considering Al_2O_3 nanoparticles. Journal of Thermal Analysis and Calorimetry, 136(6): 2477-2485. https://doi.org/10.1007/s10973-018-7901-8
[35] Atashafrooz, M., Sheikholeslami, M., Sajjadi, H., Amiri Detouei, A. (2019). Interaction effects of an inclined magnetic field and nanofluid on forced convection heat transfer and flow irreversibility in a duct with an abrupt contraction. Journal of Magnetism and Magnetic Materials, 478: 216-226. https://doi.org/10.1016/j.jmmm.2019.01.111
[36] Sajjadi, H., Atashafrooz, M. (2018). Double MRT Lattice Boltzmann simulation of 3-D MHD natural convection in a cubic cavity with sinusoidal temperature distribution utilizing nanofluid. Int. J. of Heat and Mass Trans., 126: 489-503. https://doi.org/10.1016/j.ijheatmasstransfer.2018.05.064
[37] Sajjadi, H., Amiri Delouei, A., Sheikholeslami, M., Atashafrooz, M., Succi, S. (2019). Simulation of three dimensional MHD natural convection using double MRT Lattice Boltzmann method. Physica A: Statistical Mechanics and Its Appl., 515: 474-496. https://doi.org/10.1016/j.physa.2018.09.164
[38] Atashafrooz, M., Gandjalikhan Nassab, S.A., Lari, K. (2015). Application of full-spectrum k-distribution method to combined non-gray radiation and forced convection flow in a duct with an expansion. Journal of Mechanics Science and Technology, 29(2): 845-859. https://doi.org/10.1007/s12206-015-0148-4
[39] Nadeem, S., Hussain, S.T. (2013). Flow and heat transfer analysis of Williamson nanofluid. Applied Nanoscience, 4(8): 1005-1012. https://doi.org/10.1007/s13204-013-0282-1
[40] Gorla, R.S.R., Sidawi, I. (1994). Free convection on a vertical stretching surface with suction and blowing. Applied Science Research, 52(3): 247-257. https://doi.org/10.1007/BF00853952
[41] Goyal, M., Bhargava, R. (2014). Boundary layer flow and heat transfer of viscoelastic nanofluids past a stretching sheet with partial slip conditions. Applied Nanosciences, 4(6): 761-767. https://doi.org/10.1007/s13204-013-0254-5
[42] Andersson, H.I., Hansen, O.R., Holmedal, B. (1994). Diffusion of a chemically reactive species from a stretching sheet. International Journal of Heat and Mass Transfer, 37(4): 659-664. https://doi.org/10.1016/0017-9310(94)90137-6
[43] Prasad, K.V., Sujatha, A., Vajravelu, K., Pop, I. (2012). MHD flow and heat transfer of a UCM fluid over a stretching surface with variable thermos-physical properties. Meccanica, 47(6): 1425-39. https://doi.org/10.1007/s11012-011-9526-x
[44] Mukhopadhyay, S., Arif, G.M., Wazed Ali Pk, M. (2013). Effects of transpiration on unsteady MHD flow of an UCM fluid passing through a stretching surface in the presence of a first order chemical reaction. Chinese Physics B, 22(12): 124701.

https://doi.org/10.1088/1674-1056/22/12/124701
[45] Palani, S., Kumar, B.R., Kameswaran, P.K. (2016). Unsteady MHD flow of an UCM fluid over a stretching surface with higher order chemical reaction. Ain Shams Engineering Journal, 7(1): 399-408. https://doi.org/10.1016/j.asej.2015.11.021
[46] Gorla, R., Prasanna Kumara, B.C., Gireesha, B.J., Krishnamurthy, M.R. (2016). Effects of chemical reaction and nonlinear thermal radiation on Williamson nanofluid slip flow over a stretching sheet embedded in a porous medium. Journal of Aerospace Engineering, 29(5): 04016019. https://doi.org/10.1061/(ASCE)AS.1943-5525.0000578
[47] Megahed, A.M. (2015). MHD viscous Casson fluid flow and heat transfer with second-order slip velocity and thermal slip over a permeable stretching sheet in the presence of internal heat generation/absorption and thermal radiation. The European Physical Journal Plus, 130: 81. https://doi.org/10.1140/epjp/i2015-15081-9
[48] Alama, M.S., Asiya, M., Khatun, Rahman, M.M., Vajravelu, K. (2016). Effects of variable fluid properties and thermophoresis on unsteady forced convective boundary layer flow along a permeable stretching/shrinking wedge with variable Prandtl and Schmidt numbers. International Journal of Mechanical Sciences, 105: 191-205. https://doi.org/10.1016/j.ijmecsci.2015.11.018
[49] Rahman, M.M., Rahman, M.A., Samad, M.A., Alam, M.S. (2009). Heat transfer in micropolar fluid along a non-linear stretching sheet with temperature dependent visc-osity and variable surface temperature. Internatioal Journal of Thermophysics, 30: 1649-70. https://doi.org/10.1007/s10765-009-0656-5
[50] Rahman, M.M., Eltayeb, I.A. (2011). Convective slip flow of rarefied fluids over a wedge with thermal jump and variable transport properties. International Journal of Thermal Sciences, 50(4): 468-79. https://doi.org/10.1016/j.ijthermalsci.2010.10.020

NOMENCLATURE

T	temperature
T_∞	ambient fluid temperature
μ(T)	temperature-dependent viscosity
μ_∞	ambient viscosity
k(T)	temperature dependent thermal conductivity
k_∞	ambient thermal conductivity
ε	thermal conductivity variation parameter
δ	viscosity variation parameter
R	Radiation parameter
$k*$	thermal radiation parameter
M	Magnetic field parameter
K_n	chemical reaction parameter
θ_w	temperature difference parameter
k_∞	thermal conductivity
K_p	porosity parameter
Pe	bioconvection Péclet number
σ	bioconvection constant
Sn_∞	ambient Schmidt number of microorganism
Sc_∞	ambient Schmidt number of mass
Pr_∞	ambient Prandtl number
$Slip_1$	first order slip velocity parameter
$Slip_2$	second order slip velocity parameter
$Slip_T$	slip temperature parameter
$Slip_C$	slip concentration parameter
$Slip_N$	slip microorganism parameter respectively
$u(x,y)$	the horizontal fluid velocity component
$v(x,y)$	vertical fluid velocity component